

# Formation of Oxide Phases in the System $\text{Eu}_2\text{O}_3$ - $\text{Fe}_2\text{O}_3$

---

Ristić, Mira; Nowik, Israel; Popović, Stanko; Musić, Svetozar

Source / Izvornik: **Croatica Chemica Acta, 2000, 73, 525 - 540**

Journal article, Published version

Rad u časopisu, Objavljena verzija rada (izdavačev PDF)

Permanent link / Trajna poveznica: <https://um.nsk.hr/um:nbn:hr:217:215680>

Rights / Prava: [In copyright](#)/[Zaštićeno autorskim pravom.](#)

Download date / Datum preuzimanja: **2024-08-05**



Repository / Repozitorij:

[Repository of the Faculty of Science - University of Zagreb](#)



## Formation of Oxide Phases in the System $\text{Eu}_2\text{O}_3 - \text{Fe}_2\text{O}_3$

Mira Ristić,<sup>a,\*</sup> Israel Nowik,<sup>b</sup> Stanko Popović,<sup>c</sup> and Svetozar Musić<sup>a</sup>

<sup>a</sup> Ruder Bošković Institute, P. O. Box 180, HR-10002 Zagreb, Croatia

<sup>b</sup> Racah Institute of Physics, The Hebrew University, Jerusalem, 91904 Israel

<sup>c</sup> Department of Physics, Faculty of Science, University of Zagreb,  
P. O. Box 331, HR-10002 Zagreb, Croatia

Received April 20, 1999; revised July 10, 1999; accepted July 19, 1999

Evolution of oxide phases in the  $\text{Eu}_2\text{O}_3\text{-Fe}_2\text{O}_3$  system was investigated by X-ray powder diffraction,  $^{57}\text{Fe}$  and  $^{151}\text{Eu}$  Mössbauer spectroscopy and Fourier transform infrared spectroscopy. Samples were prepared by the solid state reaction of the corresponding oxides for two molar ratios,  $\text{Eu}_2\text{O}_3 : \text{Fe}_2\text{O}_3 = 1 : 1$  and  $3 : 5$ . After heating the mixed oxide powder with molar ratio  $\text{Eu}_2\text{O}_3 : \text{Fe}_2\text{O}_3 = 1 : 1$  up to  $900^\circ\text{C}$ ,  $\text{EuFeO}_3$  and traces of  $\text{Eu}_2\text{O}_3$  were detected by XRD, while after additional heating up to  $1100^\circ\text{C}$  traces of  $\text{Eu}_3\text{Fe}_5\text{O}_{12}$  (EuIG) were also detected.  $^{57}\text{Fe}$  and  $^{151}\text{Eu}$  Mössbauer spectroscopy showed the presence of  $\text{EuFeO}_3$ . For the molar ratio  $\text{Eu}_2\text{O}_3 : \text{Fe}_2\text{O}_3 = 3 : 5$ , EuIG was formed between  $1100$  and  $1300^\circ\text{C}$ . In the sample produced at  $1300^\circ\text{C}$ , the measured hyperfine fields at the iron sites, at room temperature, were  $H_a = 495$  and  $H_d = 402$  kOe, and the hyperfine fields at the europium sites, at  $90$  K, were  $H_{\text{I}} = 631$  kOe and  $H_{\text{II}} = 572$  kOe. Europium orthoferrite was the intermediate phase in the garnet formation. Assignations of IR bands corresponding to  $\text{EuFeO}_3$  and EuIG are discussed. Mechanical activation of the mixed oxide powder was important for the formation of polycrystalline EuIG, as a single phase.

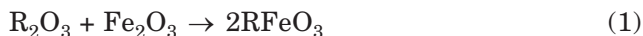
*Key words:* X-ray powder diffraction,  $^{57}\text{Fe}$  and  $^{151}\text{Eu}$  Mössbauer, FT-IR spectroscopy, europium iron garnet, europium orthoferrite

---

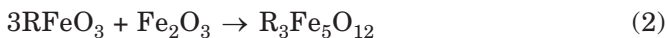
\* Author to whom correspondence should be addressed.

## INTRODUCTION

Rare earth iron garnets can be synthesized by the reaction between the oxides  $R_2O_3$ ,  $R$  = rare earth, and  $Fe_2O_3$  at high temperature. This synthesis can be described by formal chemical reactions, as follows:



The rare earth orthoferrite,  $RFeO_3$ , reacts with the additional  $Fe_2O_3$  to form the rare earth iron garnet,  $R_3Fe_5O_{12}$ :



The phase composition, microstructure and physical properties of the reaction products strongly depend on the concentration ratio of the initial reactants, the nature of the rare earth cations, temperature, as well as on other factors. In many cases it is difficult to obtain a rare earth iron garnet as a single phase. Besides the solid state synthesis of rare earth iron garnets, the researchers also focused on other methods of synthesis, such as chemical coprecipitation, thermal decomposition of mixtures of metal-organic salts, sol-gel processing, aerosol pyrolysis, crystal growth from melted glass or epitaxial growth of the films on different substrates, for example GGG (gadolinium gallium garnet).

Rare earth iron garnets, as well as substituted garnets, are important materials for advanced technologies because of their specific magnetic and magneto-optical properties. Some of them have been applied in the production of ceramic wave-guides for GHz frequencies. For this reason, knowledge of the formation of rare earth iron garnets and substituted iron garnets and the dependence of their physical properties on synthesis conditions is important for industrial technology. Various structural, spectroscopic and magnetometric methods have been used in the investigation of rare earth iron garnets. Mössbauer spectroscopy found an important application in the investigation of rare earth iron garnets.<sup>1-4</sup> In spite of the fact that garnet  $Eu_3Fe_5O_{12}$  is suitable for investigation by two active Mössbauer nuclides,  $^{151}Eu$  and  $^{57}Fe$ , the chemistry of this compound was not extensively investigated by Mössbauer spectroscopy in the past.

Nowik and Ofer<sup>5</sup> measured the  $^{57}Fe$  and  $^{151}Eu$  Mössbauer spectra of  $Eu_3Ga_xFe_{5-x}O_{12}$ ,  $0 \leq x \leq 3.03$ , at 4.2 K. The results showed that ~80% of  $Ga^{3+}$  ions occupied tetrahedral sites in the garnet. Also, it was found that ~90% of the exchange field acting on  $Eu^{3+}$  ions in EuIG was produced by the two nearest  $Fe^{3+}$  neighbours at the tetrahedral sites, in spite of the fact that the

Fe-O-Eu angle for these Fe<sup>3+</sup> ions was 92°, which is often considered unfavourable for superexchange interactions. Stachel *et al.*<sup>6</sup> also reported two magnetically inequivalent Eu<sup>3+</sup> sites in EuIG. The electric quadrupole interactions at the octahedral, tetrahedral and dodecahedral sites in garnet Eu<sub>3-y</sub>Sc<sub>2+y</sub>Fe<sub>3</sub>O<sub>15</sub>, 0 ≤ y ≤ 0.5, were also studied with <sup>57</sup>Fe and <sup>151</sup>Eu Mössbauer spectroscopy.<sup>7,8</sup> The ordering temperature  $T_N$  and the hyperfine magnetic fields at the <sup>57</sup>Fe nuclei were found to increase with an increase in y. The iron magnetic moments at the octahedral and tetrahedral sites were found to be non-collinear.

X-ray powder diffraction and Mössbauer spectroscopy were used<sup>9</sup> to investigate the samples, prepared by chemical coprecipitation in the system (1-x)Fe<sub>2</sub>O<sub>3</sub>+xEu<sub>2</sub>O<sub>3</sub>, 0 ≤ x ≤ 1. The samples produced at 600 °C contained poorly crystallized phases and an amorphous fraction, whereas the samples produced at 900 °C were well-crystallized. The phase distribution of α-Fe<sub>2</sub>O<sub>3</sub>, EuFeO<sub>3</sub>, Eu<sub>3</sub>Fe<sub>5</sub>O<sub>12</sub> and Eu<sub>2</sub>O<sub>3</sub> in dependence on x for the samples prepared at 900 °C was determined.<sup>10</sup> A similar effect was observed<sup>11,12</sup> during the formation of Er<sub>3</sub>Fe<sub>5</sub>O<sub>12</sub> from the coprecipitate 3Er(OH)<sub>3</sub>+5Fe(OH)<sub>3</sub>. The samples produced up to 650 °C were amorphous for X-ray diffraction, and the first appearance of Er<sub>3</sub>Fe<sub>5</sub>O<sub>12</sub> was observed in the sample produced at 750 °C. The <sup>57</sup>Fe Mössbauer spectrum at RT of the initial coprecipitate was characterized by a quadrupole doublet ( $\delta_{Fe} = 0.38$ ,  $\Delta = 0.80$  and  $\Gamma = 0.50$  mm s<sup>-1</sup>). Material produced at 650 °C showed superposition of two quadrupole doublets and of a sextet of very small spectral line intensity with  $H = 506$  kOe at RT. This result indicated that the amorphous phase, as detected by XRD, actually contained an additional Fe-bearing oxide phase of very fine particles, which probably exhibited poor crystallinity. Vaqueiro *et al.*<sup>13</sup> investigated the formation of Y<sub>3</sub>Fe<sub>5</sub>O<sub>12</sub> (YIG) using sol-gel processing. Crystallized YIG appeared above 650 °C and, depending on the thermal treatment, the particles size varied between 30 and 500 nm. De Souza, Jr., *et al.*<sup>14</sup> heated the coprecipitate Eu(OH)<sub>3</sub>+9Fe(OH)<sub>3</sub> between 500 and 1250 °C and after cooling to RT the samples were analyzed by XRD, DTA and Mössbauer spectroscopy. After heating at 500 °C, XRD indicated the amorphous character of the sample. A poorly resolved sextet, observed by Mössbauer spectroscopy, was assigned to α-Fe<sub>2</sub>O<sub>3</sub>. The sample produced by heating at 1250 °C contained 83% of α-Fe<sub>2</sub>O<sub>3</sub> and 13% of Eu<sub>3</sub>Fe<sub>5</sub>O<sub>12</sub>. This work<sup>14</sup> and previously reviewed works<sup>9-13</sup> indicate that the formation of α-Fe<sub>2</sub>O<sub>3</sub> from amorphous Fe(OH)<sub>3</sub> was strongly suppressed by the presence of rare earth cations. Generally, in the absence of rare earth, α-Fe<sub>2</sub>O<sub>3</sub> crystallized from amorphous Fe(OH)<sub>3</sub> with heating slightly above 200 °C.

In the present work, we focus on the formation of oxide phases by the solid state reaction between Eu<sub>2</sub>O<sub>3</sub> and α-Fe<sub>2</sub>O<sub>3</sub>. The aim of this work was

to ascertain the experimental conditions for the synthesis of EuIG as a single phase and also to characterize the oxide phases present during the process of EuIG formation. X-ray powder diffraction and two spectroscopic techniques were applied in order to solve the problems that may be present in the characterization of oxide phases in the system investigated, as well as in analogous systems, especially in the region of phase transitions.

## EXPERIMENTAL

The chemicals,  $\text{Eu}_2\text{O}_3$  and  $\alpha\text{-Fe}_2\text{O}_3$ , were of analytical purity. Before starting the experiments, the chemicals were dried and  $\text{Eu}_2\text{O}_3$  was additionally calcined to remove  $\text{H}_2\text{O}$  and carbonates. Proper weights of oxide powders were mixed and mechanically activated by ball-milling in a Fritsch planetary mill (Pulverisette 5). An agate bowl and balls (99.9%  $\text{SiO}_2$ ) were used. For mechanical activation in the present case, we do not recommend the use of bowl and balls made of other materials because there may be significant contamination of oxide powders. The mixed powders were sintered into rods and then heated in air. An LKO II furnace with Kanthal heaters was used for temperatures above 1000 °C. Experimental conditions for the preparation of samples are given in Table I.

TABLE I  
Experimental conditions for the preparation of samples

Sample	$\text{Fe}_2\text{O}_3 : \text{Eu}_2\text{O}_3$	Ball-milling time (h)	Heating temperature (°C)	Heating time (h)
E1	1 : 1	3	200	1
			300	1
			400	1
			600	5
			700	5
E2	1 : 1	1	200	1
			300	1
			400	1
			600	5
			900	6
E3	1 : 1	3	200	1
			300	1
			400	1
			1100	2

TABLE I (continued)

Sample	Fe <sub>2</sub> O <sub>3</sub> : Eu <sub>2</sub> O <sub>3</sub>	Ball-milling time (h)	Heating temperature (°C)	Heating time (h)
E4	1 : 1	3	200	1
			300	1
			400	1
			600	5
			900	6
			1100	2
E5	5 : 3	1	200	1
			300	1
			400	1
			600	5
			700	5
E6	5 : 3	1	200	1
			300	1
			400	1
			600	5
			900	6
			1100	2
E7	5 : 3	1	200	1
			300	1
			400	1
			600	5
			900	6
			1100	2
			1300	2

X-ray powder diffraction (XRD) measurements were made with a Philips diffractometer MPD 1880 (graphite monochromator, CuK $\alpha$  radiation and proportional counter).

<sup>57</sup>Fe and <sup>151</sup>Eu Mössbauer spectra were recorded with a conventional constant acceleration velocity drive spectrometer. The sources used were <sup>57</sup>Co/Rh (30 mCi) and <sup>151</sup>Sm<sub>2</sub>O<sub>3</sub> (200 mCi). Isomer shifts are given relative to  $\alpha$ -Fe and Eu<sub>2</sub>O<sub>3</sub>.

The FT-IR spectra were recorded with a spectrometer (model 2000) manufactured by Perkin-Elmer. The Infrared Data Manager (IRDM) program, also supplied by Perkin-Elmer, was used to process the recorded spectra. The specimens were pressed onto the surface of polyethylene foil.

## RESULTS AND DISCUSSION

The results of XRD phase analysis of samples E1 to E7 are summarized in Table II while the characteristic parts of X-ray powder diffraction pat-

TABLE II  
Phase composition of the samples, as determined  
by X-ray powder diffraction

Sample	Phase composition (approx. molar fraction)
E1	Eu <sub>2</sub> O <sub>3</sub> + α-Fe <sub>2</sub> O <sub>3</sub> + EuFeO <sub>3</sub> (0.4) (0.4) (0.2)
E2	EuFeO <sub>3</sub> + Eu <sub>2</sub> O <sub>3</sub> (traces)
E3	EuFeO <sub>3</sub> + Eu <sub>2</sub> O <sub>3</sub> + Eu <sub>3</sub> Fe <sub>5</sub> O <sub>12</sub> (0.03) (traces)
E4	EuFeO <sub>3</sub> + Eu <sub>2</sub> O <sub>3</sub> + Eu <sub>3</sub> Fe <sub>5</sub> O <sub>12</sub> (0.05) (traces)
E5	Eu <sub>2</sub> O <sub>3</sub> + α-Fe <sub>2</sub> O <sub>3</sub> + EuFeO <sub>3</sub> (0.4) (0.4) (0.2)
E6	Eu <sub>3</sub> Fe <sub>5</sub> O <sub>12</sub> + α-Fe <sub>2</sub> O <sub>3</sub> (traces)
E7	Eu <sub>3</sub> Fe <sub>5</sub> O <sub>12</sub>

TABLE III  
Crystallographic data for Eu<sub>2</sub>O<sub>3</sub>, EuFeO<sub>3</sub>, Eu<sub>3</sub>Fe<sub>5</sub>O<sub>12</sub> and α-Fe<sub>2</sub>O<sub>3</sub>

Compound	Space group	Unit-cell parameters	ICD PDF Card no:
Eu <sub>2</sub> O <sub>3</sub> europia	<i>I a 3</i> (206)	<i>a</i> = 10.869 Å	12-393
EuFeO <sub>3</sub>	<i>P b n m</i> (62) or <i>P b n 2</i> <sub>1</sub> (33)	<i>a</i> = 5.371 Å <i>b</i> = 5.611 Å <i>c</i> = 7.686 Å	8-407
Eu <sub>3</sub> Fe <sub>5</sub> O <sub>12</sub>	<i>I a 3 d</i> (230)	<i>a</i> = 12.496 Å	23-1069
α-Fe <sub>2</sub> O <sub>3</sub> hematite	<i>R 3̄</i> (167)	Hexagonal axes <i>a</i> = 5.034 Å <i>c</i> = 13.752 Å	13-534

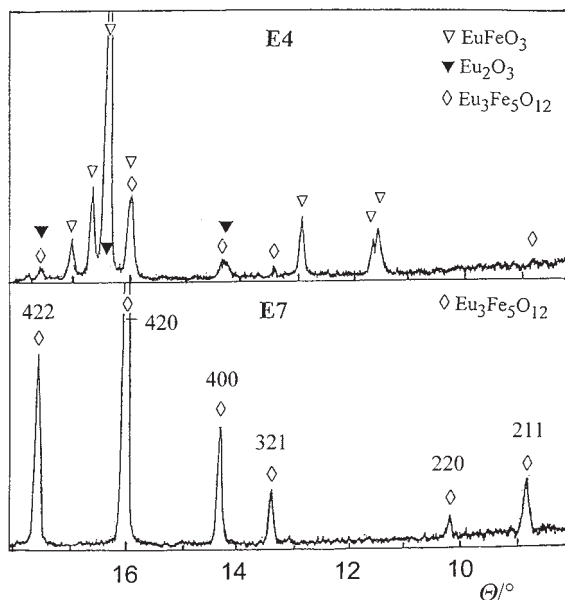


Figure 1. Characteristic X-ray powder diffraction patterns of samples E4 and E7, recorded at room temperature.

terns of samples E4 and E7 are shown in Figure 1. Table III shows crystallographic data for the phases Eu<sub>2</sub>O<sub>3</sub>, EuFeO<sub>3</sub>, Eu<sub>3</sub>Fe<sub>5</sub>O<sub>12</sub> and  $\alpha$ -Fe<sub>2</sub>O<sub>3</sub> detected in the investigated samples. The ionic radii of Fe<sup>3+</sup> and Eu<sup>3+</sup> ions are significantly different (0.67 Å for Fe<sup>3+</sup> and 0.97 Å for Eu<sup>3+</sup>) and for this reason there was no tendency to formation of solid solutions of Fe<sup>3+</sup> in Eu<sub>2</sub>O<sub>3</sub> and Eu<sup>3+</sup> in Fe<sub>2</sub>O<sub>3</sub>. Formation of solid solutions in this system can be expected only at a very small concentration of the doping compound. After heating at 700 °C the mixed oxide powder with molar ratio Fe<sub>2</sub>O<sub>3</sub> : Eu<sub>2</sub>O<sub>3</sub> = 1 : 1, equimolar amounts of starting oxides and EuFeO<sub>3</sub> were obtained. With an increase of temperature to 900 °C, EuFeO<sub>3</sub> was formed, and XRD also detected traces of Eu<sub>2</sub>O<sub>3</sub>. After heating at a maximum temperature of 1100 °C, traces of EuIG appeared in the sample, as determined by XRD. For the molar ratio Fe<sub>2</sub>O<sub>3</sub> : Eu<sub>2</sub>O<sub>3</sub> = 5 : 3, after heating at 1100 °C, EuIG and traces of  $\alpha$ -Fe<sub>2</sub>O<sub>3</sub> were detected by XRD, whereas heating at 1300 °C produced EuIG as a single phase. Evidently, EuFeO<sub>3</sub> was the intermediate phase formed prior to the formation of EuIG.

Figure 2 shows <sup>57</sup>Fe Mössbauer spectra of samples E1 to E4 recorded at room temperature. The spectrum of sample E1 was resolved into two sextets corresponding to  $\alpha$ -Fe<sub>2</sub>O<sub>3</sub> and EuFeO<sub>3</sub>. The spectra of samples E2, E3 and E4 were fitted for one sextet with the parameters corresponding<sup>15</sup> to EuFeO<sub>3</sub>. <sup>57</sup>Fe and <sup>151</sup>Eu Mössbauer parameters of selected samples are given

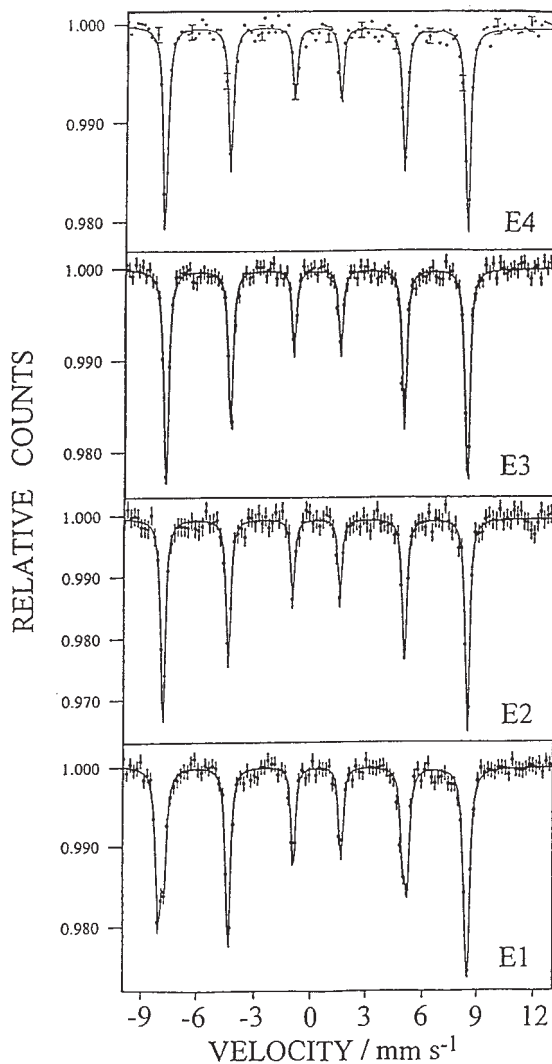


Figure 2.  $^{57}\text{Fe}$  Mössbauer spectra of samples E1 to E4, recorded at room temperature.

in Table IV. Figure 3 shows  $^{151}\text{Eu}$  Mössbauer spectra of samples E3 and E4, recorded at room temperature, and the spectrum of the pure phase  $\text{Eu}_2\text{O}_3$  is shown for comparison. These spectra indicate a single europium site in samples E3 and E4. Taking into account the result of  $^{57}\text{Fe}$  Mössbauer spectroscopy, this site can be ascribed to  $\text{EuFeO}_3$ . The  $^{57}\text{Fe}$  Mössbauer spectra of samples E5, E6 and E7 recorded at room temperature are shown in Figure 4. The spectrum of sample E5 can be considered to be the superposition of

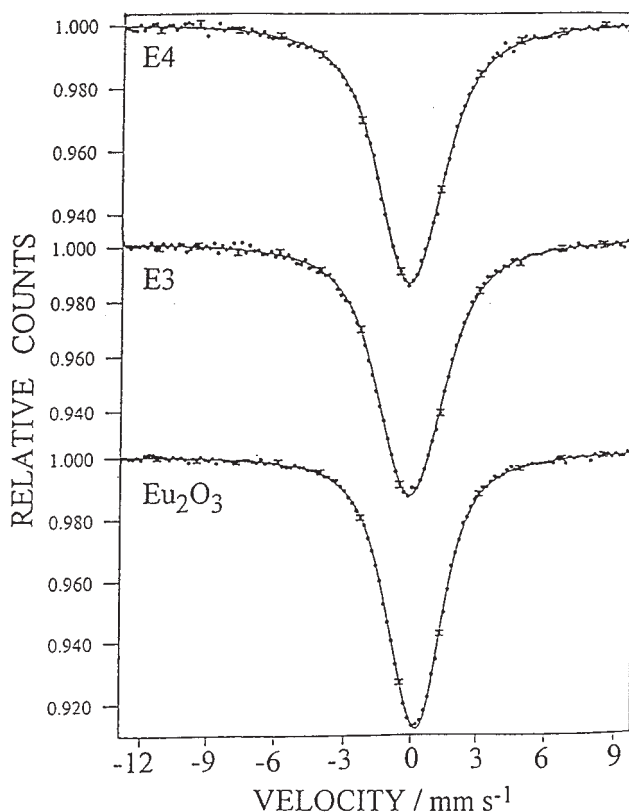


Figure 3. <sup>151</sup>Eu Mössbauer spectra of samples E3, E4 and Eu<sub>2</sub>O<sub>3</sub>, recorded at room temperature.

two sextets. This is in accordance with XRD results, which showed the presence of two Fe-bearing components,  $\alpha$ -Fe<sub>2</sub>O<sub>3</sub> and EuFeO<sub>3</sub>, in sample E5. For sample E5, the two magnetic hyperfine fields were  $H_I = 515$  kOe and  $H_{II} = 505$  kOe, well corresponding to  $\alpha$ -Fe<sub>2</sub>O<sub>3</sub> and EuFeO<sub>3</sub>, respectively. <sup>151</sup>Eu Mössbauer spectra of samples E6 and E7 are shown in Figure 5. These spectra were resolved into two subspectra corresponding to two magnetically inequivalent europium sites in EuIG. With a decrease of temperature down to 90 K, the hyperfine magnetic fields significantly increased, as shown in Table IV. These spectra also showed high symmetry, with an isomer shift near zero and relatively small quadrupole splitting. In samples E6 and E7, <sup>151</sup>Eu Mössbauer spectroscopy showed no additional Eu-bearing phases.

FT-IR spectra of samples E1 to E4 are shown in Figure 6. For the molar ratio Eu<sub>2</sub>O<sub>3</sub> : Fe<sub>2</sub>O<sub>3</sub> = 1 : 1, the spectra of samples E1 to E4 are similar. The IR band at 476 cm<sup>-1</sup> is more pronounced for sample E1 than for other sam-

TABLE IV  
 $^{57}\text{Fe}$  and  $^{151}\text{Eu}$  Mössbauer parameters of selected samples

Sample	Mössbauer nuclide	Temp.	Spectral lines	$IS$ (mm s $^{-1}$ )	$e_{\text{qq}}/4$ (mm s $^{-1}$ )	$H_{\text{eff}}$ (kOe)	Relative intensity
E1	$^{57}\text{Fe}$	RT	I	0.33	-0.10	514	0.59
			II	0.33	0.00	499	0.41
	$^{151}\text{Eu}$	RT	I	0.00	-1.30		0.65
			II	-0.20	-1.60		0.35
E2	$^{57}\text{Fe}$	RT		0.31	0.00	504	1
	$^{151}\text{Eu}$	RT		0.00	-1.70		1
E5	$^{57}\text{Fe}$	RT	I	0.32	-0.10	515	0.67
			II	0.26	0.03	505	0.33
E6	$^{57}\text{Fe}$	RT	I	0.13	0.00	402	0.60
			II	0.35	0.00	494	0.40
	$^{151}\text{Eu}$	90 K	I	-0.50	-0.50	630	0.50
			II	-0.50	+0.50	567	0.50
E7	$^{57}\text{Fe}$	RT	I	0.13	0.00	402	0.58
			II	0.35	0.00	495	0.42
	$^{151}\text{Eu}$	RT	I	-0.80	-0.10	355	0.50
			II	-0.80	+0.10	305	0.50
		90 K	I	-0.50	-0.50	631	0.50
			II	-0.50	+0.50	572	0.50

Errors for  $^{57}\text{Fe}$ :  $\delta = \pm 0.01$  mm s $^{-1}$ ,  $e_{\text{qq}} = \pm 0.01$  mm s $^{-1}$ ,  $H_{\text{eff}} = \pm 2$  kOe  
 Errors for  $^{151}\text{Eu}$ :  $\delta = \pm 0.1$  mm s $^{-1}$ ,  $e_{\text{qq}} = \pm 0.1$  mm s $^{-1}$ ,  $H_{\text{eff}} = \pm 6$  kOe

Key:  $IS$  = isomer shifts relative to  $\alpha\text{-Fe}$  and  $\text{Eu}_2\text{O}_3$ ;  $e_{\text{qq}}$  = electric quadrupole splitting;  $H_{\text{eff}}$  = hyperfine magnetic field

ples, whereas the bands at 321 and 294 are strongly suppressed. The positions of the bands at 551, 476, 381, and 354 cm $^{-1}$ , observed for sample E1 correspond<sup>16</sup> to  $\alpha\text{-Fe}_2\text{O}_3$ ; however, these IR bands are overlapped with those of  $\text{EuFeO}_3$  and  $\text{Eu}_2\text{O}_3$  phases, which were detected by XRD. The IR bands, recorded for sample E4 at 553, 476, 425, 387 and 357 cm $^{-1}$  and three bands of small intensity at 321, 309 and 292 cm $^{-1}$  can be due to the presence of  $\text{EuFeO}_3$ . In previous research<sup>17</sup> of the analogous  $\text{Sm}_2\text{O}_3 : \text{Fe}_2\text{O}_3$  system, the IR bands at 555, 440 to 415, 380, 350, 305 and 285 cm $^{-1}$  were recorded. Lu

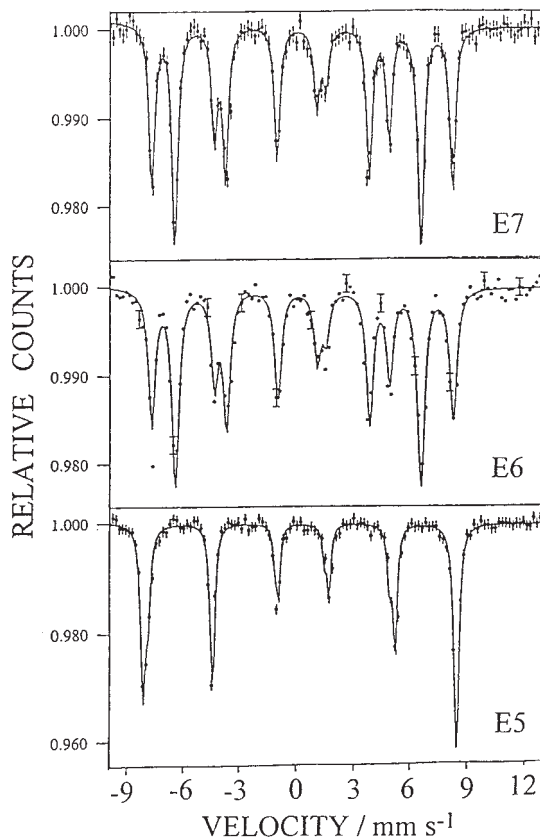


Figure 4. <sup>57</sup>Fe Mössbauer spectra of samples E5, E6 and E7, recorded at room temperature.

and Hofmeister<sup>18</sup> reported assignments of IR bands for CaGeO<sub>3</sub> with a metastable orthorhombic perovskite structure at a pressure up to 24.4 GPa. The IR reflectance spectrum showed 18 IR modes from 155 to 786 cm<sup>-1</sup>. Saine and Husson<sup>19</sup> reported spectra of some rare earth aluminates including EuAlO<sub>3</sub>.

FT-IR spectra of samples E6 and E7 in Figure 7 show the main features of the garnet structure. Generally, the rare earth iron garnets can be described by the chemical formula, {R<sub>3</sub><sup>3+</sup>}<sub>c</sub>[Fe<sub>2</sub><sup>3+</sup>]<sub>a</sub>(Fe<sub>3</sub><sup>3+</sup>)<sub>d</sub>O<sub>12h</sub><sup>2-</sup>, where different types of brackets and subscripts *a*, *c*, *d*, and *h* indicate different cation coordinations and different Wyckoff positions, respectively.<sup>20</sup> The rare earth cations {R<sub>3</sub><sup>3+</sup>}<sub>c</sub> in the twenty-four dodecahedral positions are surrounded by eight oxygen anions. The iron cations [Fe<sub>2</sub><sup>3+</sup>]<sub>a</sub> in the sixteen octahedral positions and iron cations (Fe<sub>3</sub><sup>3+</sup>)<sub>d</sub> in the twenty-four tetrahedral positions have

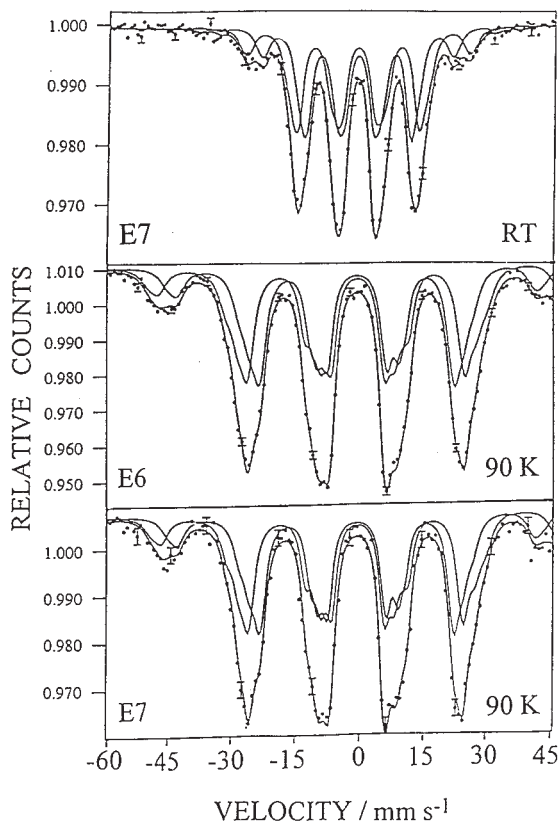


Figure 5.  $^{151}\text{Eu}$  Mössbauer spectra of samples E6 and E7.

oxygen coordination numbers 6 and 4, respectively. The garnet structure belonging to the space group ( $Ia\bar{3}d$ ) (230) exhibits 17 triply degenerate  $T_{1u}$  modes that are active in the infrared region.<sup>21</sup> If the vibrational motions of the tetrahedron are mildly perturbed by placing this unit in the garnet structure, these 17 IR modes should consist of three asymmetric stretching modes of the tetrahedron  $\nu_3$ , three asymmetric bending modes  $\nu_4$ , one symmetric bend  $\nu_2$ , two rotations (librations)  $R$  of the tetrahedron, two translations  $T$  of the tetrahedron, three translations  $T_d$  of the dodecahedral cations, and two translations  $T_o$  of the octahedral cations. All 17 IR modes were monitored<sup>22</sup> in the spessartine ( $\text{Mn}_3\text{Al}_2\text{Si}_3\text{O}_{12}$ )-yttrium aluminium garnet ( $\text{Y}_3\text{Al}_2\text{Al}_3\text{O}_{12}$ ) system. Also, Hofmeister and Chopelas<sup>23</sup> recorded IR and Raman spectra for 5 natural garnets: pyrope ( $\text{Mg}_3\text{Al}_2\text{Si}_3\text{O}_{12}$ ), almandine ( $\text{Fe}_3\text{Al}_2\text{Si}_3\text{O}_{12}$ ), spessartine ( $\text{Mn}_3\text{Al}_2\text{Si}_3\text{O}_{12}$ ), grossular ( $\text{Ca}_3\text{Al}_2\text{Si}_3\text{O}_{12}$ ) and andradite ( $\text{Ca}_3\text{Fe}_2\text{Si}_3\text{O}_{12}$ ). Assignments were made for all 17 IR modes and all 25 Raman modes. However, not all researchers observed all 17 IR modes in

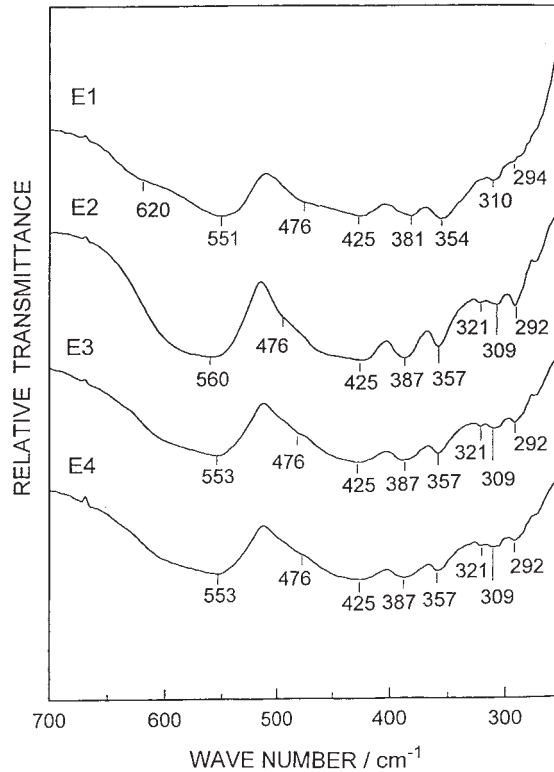


Figure 6. FT-IR spectra of samples E1 to E4, recorded at room temperature.

the garnets. For example, Hurrell *et al.*<sup>24</sup> observed 15 IR modes for YAG using IR reflectance spectroscopy on a single crystal. Powder absorption IR spectra of YAG showed 16 bands at room temperature and 24 bands at liquid helium temperature.<sup>25</sup> Beregi and Hild<sup>26,27</sup> investigated the IR spectra of garnets,  $R_3Fe_{5-x}Ga_xO_{12}$ ,  $R = Y, Sm, Gd, Er, Yb, Lu$ , and they ascribed a broad and very strong band at  $\sim 600\text{ cm}^{-1}$  to the vibration of isolated tetrahedra, whereas a very strong band at  $\sim 400\text{ cm}^{-1}$  was ascribed to isolated octahedra. In the present work, the FT-IR spectrum of EuIG (sample E7) showed three IR bands as 636, 586 and  $550\text{ cm}^{-1}$  corresponding to  $\nu_3$  modes in the garnet. The same sample also showed IR bands at 428, 375, 357, 327, 310 and  $255\text{ cm}^{-1}$ . The IR band at  $428\text{ cm}^{-1}$  can be ascribed to the  $\nu_4$  mode, and the bands at 375 and  $357\text{ cm}^{-1}$  can be ascribed to the  $\nu_4$  and  $\nu_2$  modes, respectively. In accordance with the work of Hofmeister and Campbell,<sup>21</sup> the broad IR band at  $327\text{ cm}^{-1}$  corresponds to the  $T_o$  mode, whereas the bands at 310 and  $255\text{ cm}^{-1}$  cannot be ascribed with certainty to  $R$  modes in the EuIG.

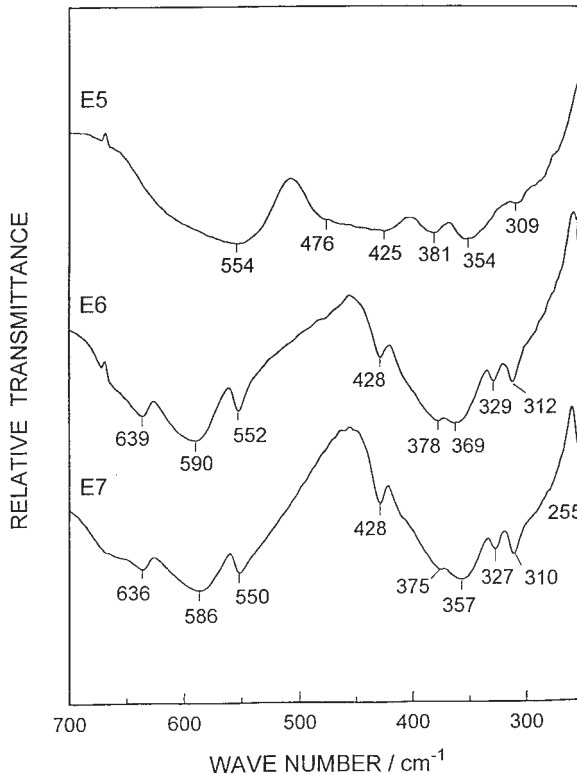


Figure 7. FT-IR spectra of samples E5 to E7, recorded at room temperature.

## CONCLUSIONS

Formation of oxide phases in the  $\text{Eu}_2\text{O}_3\text{-Fe}_2\text{O}_3$  system was strongly dependent on the experimental conditions, such as initial  $\text{Eu}_2\text{O}_3/\text{Fe}_2\text{O}_3$  molar ratio, temperature, and mechanical activation of the mixture of oxide powders. An agate bowl and balls (99.9%  $\text{SiO}_2$ ) were used. Use of other materials is not recommended for the ball-milling operation because there may be significant contamination of the oxide powders. The ceramic procedure was used in the preparation of samples.

For the molar ratio  $\text{Eu}_2\text{O}_3 : \text{Fe}_2\text{O}_3 = 1 : 1$ , the heating of mixed oxide powder up to  $900^\circ\text{C}$  led to formation of  $\text{EuFeO}_3$  and traces of  $\text{Eu}_2\text{O}_3$ , as detected by XRD while, after heating up to  $1100^\circ\text{C}$ ,  $\text{EuIG}$  traces were additionally detected. However,  $^{57}\text{Fe}$  and  $^{151}\text{Eu}$  Mössbauer spectroscopy revealed the presence of  $\text{EuFeO}_3$  in these samples.

For the molar ratio  $\text{Eu}_2\text{O}_3 : \text{Fe}_2\text{O}_3 = 3 : 5$ ,  $\text{EuIG}$  was obtained between  $1100$  and  $1300^\circ\text{C}$ . Hyperfine magnetic fields at iron sites of  $\text{EuIG}$ , obtained

as a single phase, were  $H_a = 495$  and  $H_d = 402$  kOe, whereas the hyperfine fields at europium sites, at 90 K, were  $H_I = 631$  kOe and  $H_{II} = 572$  kOe. <sup>151</sup>Eu Mössbauer spectra of EuIG showed high symmetry, with an isomer shift near zero and relatively small quadrupole splitting. Europium orthoferrite was the intermediate phase in the EuIG formation. The main IR bands recorded for the EuIG were interpreted in accordance with the vibrational spectroscopy of the garnets.

## REFERENCES

1. S. Musić, *Mössbauer Spectroscopic Characterization of Mixed Oxides Containing Iron Ions*, in: N. P. Cheremisinoff (Ed.), *Handbook of Ceramics and Composites*, Vol. 2, M. Dekker, Inc., New York-Basel-Hong Kong, 1992, Chap. 11, pp. 423–463.
2. F. J. Berry, J. Davalos, C. Greaves, J. F. Marco, M. Slaski, P. R. Slater, and M. Vithal, *J. Solid State Chem.* **115** (1995) 435–440.
3. F. J. Berry, J. Z. Davalos, J. R. Gancendo, C. Greaves, J. F. Marco, R. Slater, and M. Vithal, *J. Solid State Chem.* **122** (1996) 118–129.
4. J. Tejada, X. X. Zhang, F. J. Berry, and G. Dates, *J. Magn. Magn. Mater.* **140** (1995) 2165–2166.
5. I. Nowik and S. Ofer, *Phys. Rev.* **153** (1967) 409–415.
6. M. Stachel, S. Hübner, G. Creelius, and D. Quitmann, *Phys. Rev.* **186** (1969) 355–360.
7. Z. M. Stadnik and B. F. Otterloo, *J. Solid State Chem.* **48** (1983) 133–141.
8. Z. M. Stadnik, *J. Magn. Magn. Mater.* **37** (1983) 138–146.
9. M. Ristić, S. Popović, and S. Musić, *J. Mater. Sci. Lett.* **9** (1990) 872–875.
10. M. Ristić, S. Popović, I. Czakó-Nagy, and S. Musić, *Mater. Lett.* **27** (1996) 337–341.
11. M. Ristić, I. Czakó-Nagy, S. Popović, S. Musić, A. Vértes, and M. Ivanda, *J. Molec. Struct.* **410–411** (1997) 281–284.
12. M. Ristić, S. Popović, S. Musić, I. Czakó-Nagy, A. Vértes, M. Maiorov, and A. Petrov, *J. Alloys & Comp.* **256** (1997) 27–33.
13. P. Vaqueiro and M. A. López-Quintela, *Chem. Mater.* **9** (1997) 2836–2841.
14. P. A. de Souza, Jr., R. Garg, M. F. de Jesus Filho, G. P. Santana, V. K. Garg and I. Nowik, *Proceedings of the ICAME-95*, I. Ortalli (Ed.), Rimini, Italy, 1995.
15. M. Eibschütz, G. Gorodetsky, S. Shtrikman, and D. Treves, *J. Appl. Phys.* **35** (1964) 1071–1072.
16. M. Gotić, S. Popović, N. Ljubešić, and S. Musić, *J. Mater. Sci.* **29** (1994) 2474–2480.
17. M. Ristić, S. Popović, I. Czakó-Nagy, and S. Musić, *Croat. Chem. Acta* **67** (1994) 315–326.
18. R. Lu and A. M. Hofmeister, *Phys. Chem. Miner.* **21** (1994) 78–84.
19. M. C. Saine and E. Husson, *Spectrochim. Acta* **40A** (1984) 733–738.
20. A. Seidel, L. Häggström, and D. Rodić, *Hyp. Interact.* **73** (1992) 265–275.
21. A. M. Hofmeister and K. R. Campbell, *J. Appl. Phys.* **72** (1992) 638–646.
22. R. Lu, K. D. Jackson, and A. M. Hofmeister, *Canad. Miner.* **31** (1993) 381–390.
23. A. M. Hofmeister and A. Chopelas, *Phys. Chem. Miner.* **17** (1991) 503–526.
24. J. P. Hurrell, S. P. S. Porto, I. F. Chang, S. S. Mitra, and P. P. Bauman, *Phys. Rev.* **173** (1968) 851–856.

25. G. A. Slack, D. W. Oliver, R. M. Chrenko, and S. Roberts, *Phys. Rev.* **177** (1969) 1308–1314.
26. E. Beregi and E. Hild, *Acta Phys. Hung.* **61** (1987) 235–238.
27. E. Beregi and E. Hild, *Phys. Scr.* **40** (1989) 511–513.

## SAŽETAK

### Nastajanje oksidnih faza u sustavu $\text{Eu}_2\text{O}_3\text{-Fe}_2\text{O}_3$

*Mira Ristić, Israel Nowik, Stanko Popović i Svetozar Musić*

Istraživano je nastajanje oksidnih faza u sustavu  $\text{Eu}_2\text{O}_3\text{-Fe}_2\text{O}_3$  primjenom rentgenske difrakcije na prahu,  $^{57}\text{Fe}$  i  $^{151}\text{Eu}$  Mössbauerove spektroskopije te FT-IR spektroskopije. Uzorci su pripremljeni kemijskom reakcijom u čvrstom stanju odgovarajućih oksida za dva množinska odnosa,  $\text{Eu}_2\text{O}_3 : \text{Fe}_2\text{O}_3 = 1 : 1$  i  $3 : 5$ . Nakon žarenja oksidnog praha do  $900^\circ\text{C}$  pri početnom množinskom odnosu  $\text{Eu}_2\text{O}_3 : \text{Fe}_2\text{O}_3 = 1 : 1$ , rentgenskom difrakcijom u uzorku detektirani su  $\text{EuFeO}_3$  i tragovi  $\text{Eu}_2\text{O}_3$ . Nakon dodatnog žarenja pri  $1100^\circ\text{C}$  detektirani su i tragovi  $\text{Eu}_3\text{Fe}_5\text{O}_{12}$  (EuIG).  $^{57}\text{Fe}$  i  $^{151}\text{Eu}$  Mössbauerova spektroskopija je, međutim, pokazala samo prisutnost  $\text{EuFeO}_3$ . EuIG je dobiven za molni odnos  $\text{Eu}_2\text{O}_3 : \text{Fe}_2\text{O}_3 = 3 : 5$  pri temperaturama od  $1100$  do  $1300^\circ\text{C}$ . U uzorku dobivenomu pri  $1300^\circ\text{C}$  izmjerena su hiperfina magnetna polja za ione željeza pri sobnoj temperaturi,  $H_a = 495$  kOe i  $H_d = 402$  kOe, te ione europija pri  $90$  K,  $H_I = 631$  kOe i  $H_{II} = 572$  kOe.  $\text{EuFeO}_3$  je dobiven kao međufaza tijekom nastajanja EuIG. Interpretirani su FT-IR spektri pripremljenih uzoraka. Mehanička aktivacija početne smjese oksida bila je bitna za nastajanje EuIG kao čiste faze.